ICSOS 2014 – International Conference on Space Optical Systems and Applications, May 7-9, 2014, Kobe, Japan

Lunar Optical Communications Link (LOCL): Measurements of Received Power Fluctuations and Wavefront Quality

Dirk Giggenbach
Peter Becker
Ramon Mata-Calvo
Christian Fuchs

Institute of Communications and Navigation (IKN)
German Aerospace Center (DLR)
82234 Wessling, Germany
dirk.giggenbach@dlr.de

Zoran Sodnik
Igor Zayer

European Space Agency (ESA)

***Abstract*—During the laser communication link experiments between NASA's LADEE and ESA's optical ground station on Tenerife island, DLR-IKN carried out received-power measurements using a highly sensitive power detector, and wavefront quality analysis using the focal speckle pattern method. This paper reports on the evaluation of power fluctuation statistics and wave-front quality under varying elevations, times of day, and lunar background light**

Keywords—Lunar Optical Communication Link; atmospheric intensity scintillation; wavefront quality measurement

I. INTRODUCTION

In September 2013 NASA launched the Lunar Atmosphere and Dust Environmental Explorer (LADEE) spacecraft, which is equipped with an optical communication terminal to demonstrate up to 622 Mbps downlink data [1]. This Lunar Laser Communication Demonstrator project (LLCD) utilizes a communication wavelength of 1550 nm and a pulse position modulation format. Three Optical Ground Stations (White Sands, Table Mountain, and ESA-OGS at Izaña on Tenerife) are used for communication tests with the Laser Communication Space Terminal (LLST). DLR-IKN has joined in the campaign with ESA (called LOCL – Lunar Optical Communication Link) to perform measurements of received power fluctuations and of focal speckle patterns for evaluation of the atmospheric impact onto wave-front quality.

II. LINK SCENARIO AND MEASUREMENT SETUP

A. *LOCL-downlink campaign*

OGS Transmitter Design:

The transmitter/receiver design is bi-static and was driven by the assumption that only a geometrical separation between the transmitters and the receiver could prevent cross-talk [2].

As shown in Fig. 1 at the right the transmit laser light is generated by DFB laser diodes located in a rack together with the data modulators (Photline). It also contains uplink data generation and ranging electronics (Axcon). The rack itself is located in a passively temperature stabilised room and the laser light is routed via single mode fibres to three fibre amplifiers that are mounted to the side of the telescope tube. Each amplifier can generate a maximum output power of 40 Watts, which is transmitted from 3 aperture with 40 mm diameter arranged around the aperture of the 1 meter receive telescope.

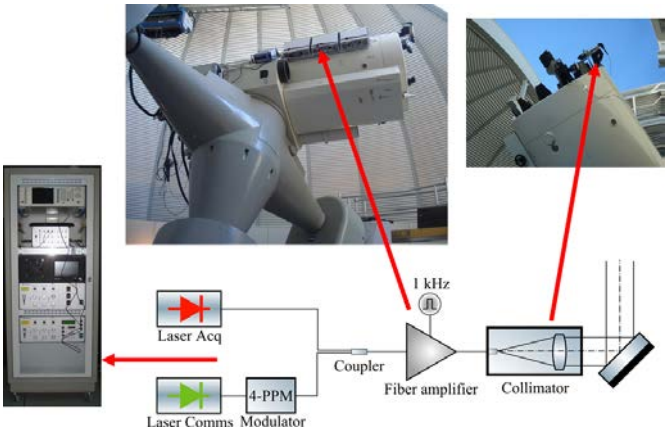

Fig. 1. Block diagram of each of the three laser transmitters used for LOCL.

OGS Receiver Design:

To cope with the weak signal irradiance from LLST the OGS optical receiver design was driven by the need to minimize transmission losses. The receiver system is therefore installed in the Cassegrain focus, where the least number of optical elements are present in the telescope (2 reflective surfaces, namely primary and secondary mirror). As shown in

Fig. 2 the focal plane instrumentation does not include a collimator, but routes the converging beam from the telescope via a filter wheel (where two narrow band-pass interference filters can be selected with 2.4 nm and 5 nm FWHM bandwidth), a tip/tilt fast steering mirror (FSM) to adjust the point ahead angle (PAA), a computer-rotated quarter-wave plate (QWP) and a polarizing beam splitter (PBS) to the acquisition and tracking camera (ACT) and the receiver fibre. The circularly polarised receive beam enables adjustment of the power ratio between the ATC and the detector fibre via the QWP and PBS pair.

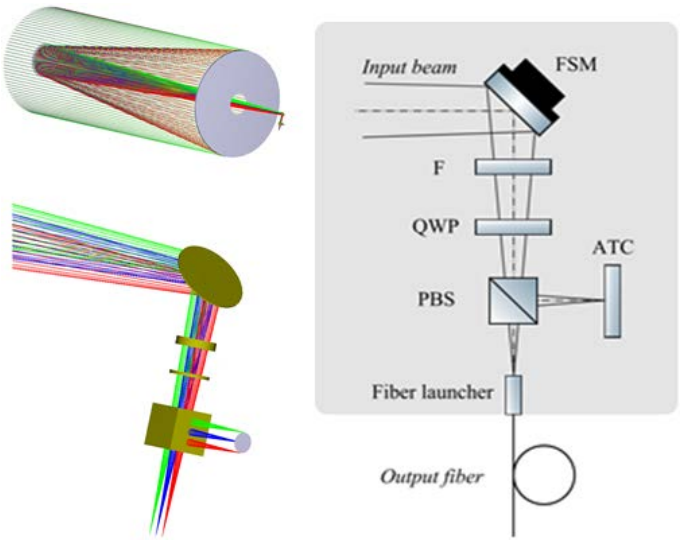

Fig. 2. Block diagram of the LOCL receiver system.

The output fibre is a 200 µm core-diameter graded-index multimode fibre, which is routed to the same passively temperature stabilized room, where the transmitter rack is located. Fig. 3 shows the detection, demodulation and storage system (RUAG Space AG Zürich).

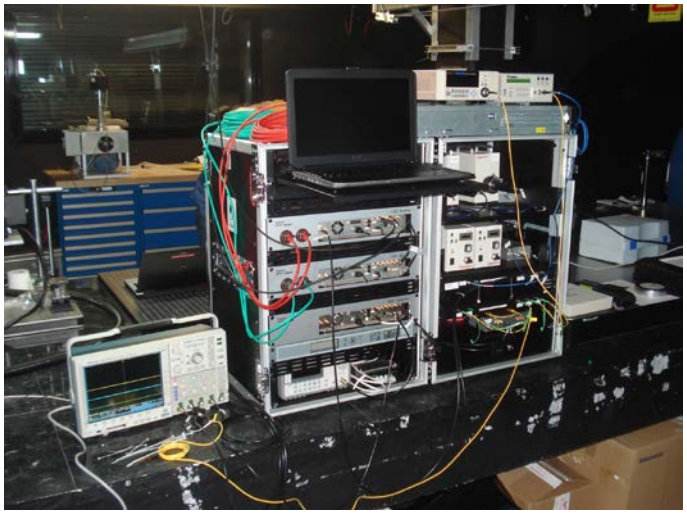

Fig. 3. Detector, demodulation and data storage system (RUAG Space).

B. Power measurements at ESA-OGS

In order to measure the received power, a high sensitivity InGaAs-Sensor (Newport/New Focus, Model 2153) was installed at one of the 20 cm guider telescopes which are coaligned to the 1 m main telescope of the ESA-OGS. A suitable set of adapters was assembled to hold a 2.4 nm band pass filter, an adjustable iris and the sensor. The detector signal was recorded together with a timestamp by means of a USB-oscilloscope (PicoScope 4424). Although the bandwidth of the sensor was 750 Hz, measurements were recorded at 10 kHz sampling rate and 12 bit resolution. Prior to the measurement campaign on Tenerife, the required sub-picowatt sensitivity of the power sensor was confirmed in a laboratory setup.

Correct alignment of the sensor was achieved by replacing the sensor with a camera and centering and focusing a star in the middle of the picture. Due to the diameter of the active area of the sensor, and the large resulting field of view, alignment proved to be uncritical for the performance of the sensor.

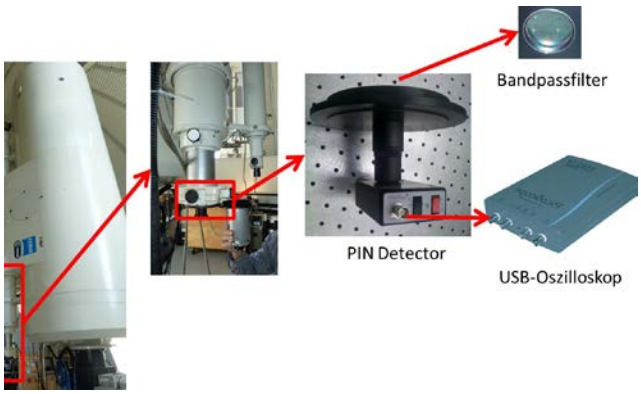

Fig. 4. Power-sensor installation at the 20cm side-telescope of the ESA-OGS, to measure received power fluctuations.

TABLE I. PARAMETER SUMMARY OF POWER SENSOR

parameter	*unit*	*value*
telescope aperture size diameter	mm	200
telescope focal length	m	3.042
optical detector diameter	mm	1
optical bandpass filter FWHM	nm	2.4
minimum sensitivity = noise amplitude	pW	1
power sensor bandwidth	Hz	750
measured mean received signal power-range min/typ/max	pW	8/18/24
measured background light offset (max)	pW	120

C. Wavefront statistics by focal speckle pattern evaluation

To estimate the downlink Fried-parameter during LOCL-links, the focal speckle size method [3] was applied, using the 1m telescope aperture of the ESA-OGS. The same camera used

for tracking the position of LADEE (ATC in Fig. 2) also provided the focal speckle pattern samples, which were then processed to estimate short- and long-term wavefront statistics.

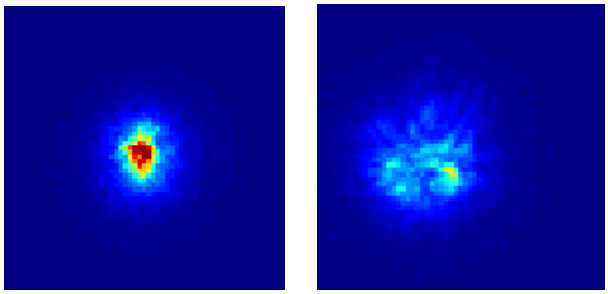

Fig. 5. Examples of typical small (left) and large (right) instantenious focal speckle patterns measured by the tracking camera in the focus of the 1m OGS telescope. The pictures show a 1.3 x 1.3 mm^2 region of the camera sensor.

The parameters of the optical system are summarized in TABLE II.

TABLE II. PARAMETER SUMMARY OF FOCAL CAMERA

parameter	*unit*	*value*
outer aperture size diameter	mm	1016
secondary obscuration diameter	mm	330
telescope focal length	m	13.3
diffraction limited speckle FWHM	µm	20.8
camera pixel resolution		640 x 512
pixel size	µm	20
exposure time	ms	5
frame rate	Hz	10 to 20

III. TURBULENCE PROFILE AND ANALYTICAL LINK ASSESSMENT

A. C_n^2-profiles for ESA-OGS at Izana

The structure parameter of the index-of-refraction turbulence describes the turbulence strength of the atmosphere. At lower altitudes the atmosphere is denser and the impact of the turbulence is therefore higher. There are several profiles which describe the behavior of the structure parameter as function of the height, but one of the most commonly used models is the Hufnagel-Valley profile (HV), which is valid at sea level. In this particular case, the ground station is located at $H_{OGS} = 2370$ meters over the sea. Just truncating the HV profile leads to an underestimation of the turbulence strength, thus a modification is introduced to consider the ground station altitude. This model is then called the modified Hufnagel-Valley (MHV) [4].

$$C_n^2(h) = 0.00594\left(v/27\right)^2 \left(10^{-5}h\right)^{10} e^{-h/1000} + \\ + 2.7\cdot 10^{-16} e^{-h/500} + A_0 e^{-H_{OGS}/700} e^{-(h-H_{OGS})/100} \quad (1)$$

h is the altitude vector in meters, v is the RMS cross wind velocity and A_0 is the ground level structure parameter value.

For the theoretical modelling two other models are available: the Izaña Day Model (IDM) and the Izaña Night Model (INM). These two models are based on in-situ measurements carried on in a campaign at the OGS, which took place in 1995 [5]. All three models are depicted in C_n^2 profiles: Modified Hufnagel-Valley (MHV), Izaña Night Model (INM) and Izaña Day Model (IDM) .

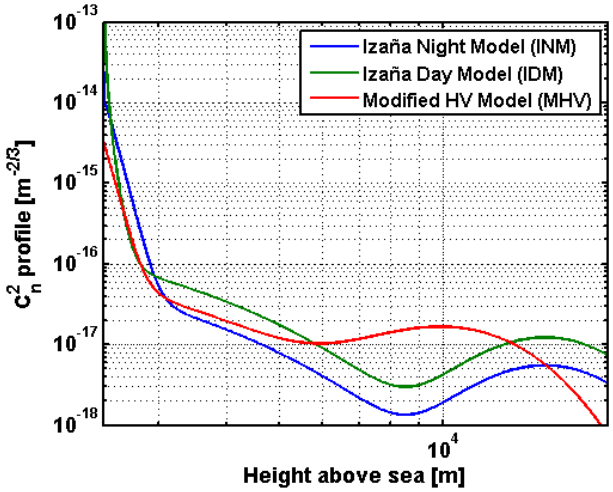

Fig. 6. C_n^2 profiles: Modified Hufnagel-Valley (MHV), Izaña Night Model (INM) and Izaña Day Model (IDM)

B. Expected Scintillation Parameter Ranges

The range distance is between 362,570 km and 405,410 km and the expected mean power irradiance from LLST at the border of the atmosphere is between 0.17 and 1.7 nW/m^2 [10]. After transmitting through the atmosphere and taking the RX optic losses and the atmospheric transmission into account, the expected received power is around 20 pW at the focus of the 20 cm telescope.

The scintillation index is the normalized variance of the irradiance fluctuations due to beam self-interference produced after propagating through the turbulent atmosphere. For a general turbulence conditions, the following formulation can be used, where σ_R^2 is the Rytov variance in case of a slant-path downlink [6].

$$\sigma_I^2 = \exp\left[\frac{0.49\sigma_R^2}{\left(1+1.11\sigma_R^{12/5}\right)^{7/6}} + \frac{0.51\sigma_R^2}{\left(1+0.69\sigma_R^{12/5}\right)^{5/6}}\right] \quad (2)$$

In Fig. 7, the scintillation values above 20° elevation remain under 0.2 and they increase for lower elevation angles, as expected.

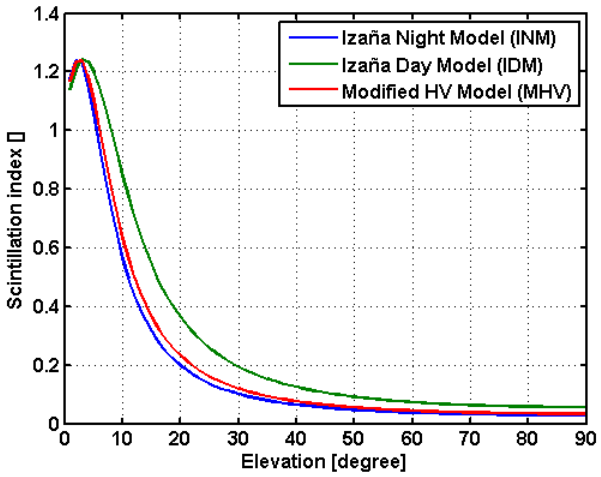

Fig. 7. Scintillation index for the three profile models

The telescope aperture is larger than the intensity distortions. This leads to aperture averaging, which is a scintillation reduction at the telescope focus, the so-called power scintillation. The following expression assumes a plane-wave model [6].

$$\sigma_I^2\left(D_G\right) = 8.70k^{7/6}\left(H-H_{OGS}\right)^{5/6}\sec^{11/6}\left(\zeta\right) \cdot \mathrm{Re}\int_{h_0}^{H} C_n^2\left(h\right)\left[\left(\frac{kD_G^2}{16L}+i\frac{h-H_{OGS}}{H-H_{OGS}}\right)^{5/6}-\left(\frac{kD_G^2}{16L}\right)^{5/6}\right]dh \quad (3)$$

k is the wave number, D_G is the telescope diameter, H is the satellite altitude, L is the link distance and ζ is the zenith angle in radians.

In Fig. 8, the power scintillation is shown. The aperture averaging reduces the signal fluctuations and after the 20 cm telescope, scintillation values between 10^{-2} and 10^{-1} are expected.

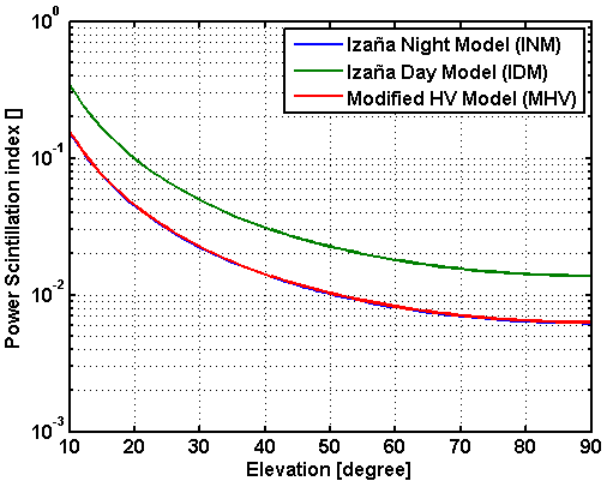

Fig. 8. Power scintillation index for the three profile models

C. *Expected Fried parameters and short-term wavefront statistics*

The Fried parameter is a measurement of the coherence length of the phase distortion on the beam transversal plane. It is generally calculated for downlink and it is compared to telescope aperture diameter. For telescope diameters greater than the Fried parameter, adaptive optics will be required if single-mode fiber coupling or a coherent receiver is used. It is therefore also a measurement of the turbulence impact on the received beam.

The distance of the laser source to the atmosphere is large enough to assume the plane-wave model for such a calculation [6].

$$r_0 = \left[0.42\sec\left(\zeta\right)k^2\int_{h_0}^{H} C_n^2\left(h\right)dh\right]^{-3/5} \quad (4)$$

In Fig. 9, the Fried parameter is depicted with respect to the elevation angle. Values decrease with the elevation angle, as expected, since the beam propagates through a larger amount of atmosphere.

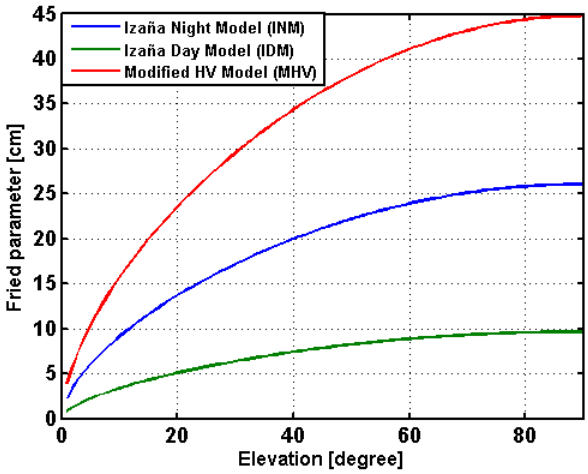

Fig. 9. Fried parameter versus elevation angle for the three profile models: MHV, INM and IDM

IV. Measured Trials and Parameter Ranges

Trials with the power-sensor and focal wavefront measurements were carried out on 26. – 29. October 2013. Additional power measurements took place in a second campaign on 18. – 19. November 2013.

A. Times and elevations of successful data takes

Power measurements were taken during the whole link (between 15 – 45 minutes) and evaluated for useful sequences afterwards. Tracking camera videos were recorded when possible. In TABLE III. a summary of all measurement sequences is given.

TABLE III. Overview of Measurements

Date-Time (UTC)	*Elevation [deg]*
2013-10-26 – 06:30	77
2013-10-26 – 10:10	38
2013-10-27 – 03:30	42
2013-10-27 – 06:15	71
2013-10-28 – 03:45	29
2013-10-28 – 10:10	54
2013-10-29 – 03:40	25
2013-10-29 – 06:20	52
2013-11-18 – 21:10	25
2013-11-18 – 22:50	48
2013-11-19 – 00:20	67

B. Parameter ranges of received power

Four suitable measurements were identified for detailed analysis (see TABLE IV.). As can be seen in Fig. 11, the received power from lunar background light can reach up to 100 pW while the Rx power levels are in the range 9 to 25 pW at 0.5 W Tx-power.

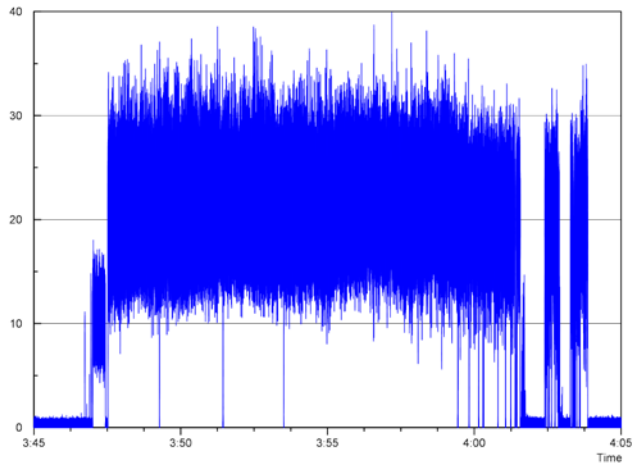

Fig. 10. Received power in pW, without lunar background light. Abscissa is UTM-time.

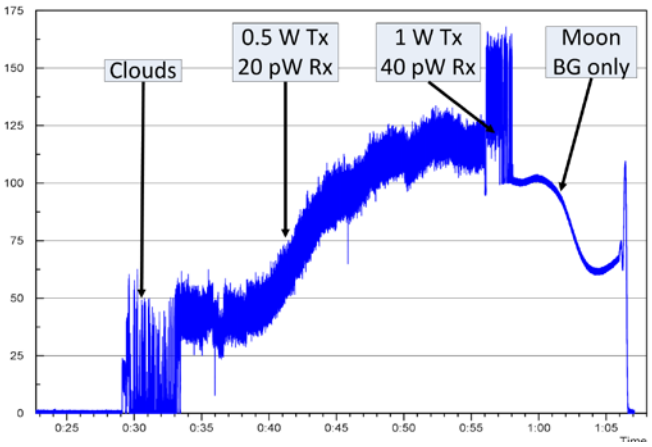

Fig. 11. Received power in pW during transit above the sun-illuminated lunar surface with varying background intensity.

TABLE IV. summarizes the power vector measurements and compares with PSI as derived from the theoretical C_n^2-profiles Izaña-Day and Izaña-Night (fifth column). It is believed, that due to the limited field of view of the power sensor, telescope misalignment and/or tracking errors the measured PSI is higher than expected in some samples.

TABLE IV. MEAN POWER AND PSI

Date – Time [UTC]	*Elevation [deg]*	*Mean Rx power [pW]*	*PSI*	*PSI from models*
2013-10-26 – 10:10	38	9.5	0.06	0.03
2013-10-27 – 03:35	40	20.9	0.03	0.015
2013-10-27 – 06:15	70	24.4	0.01	0.007
2013-11-19 – 00:24	67	18.9	0.03	0.008

PSI: power-scintillation-index

C. Parameter ranges of wavefront distortions

There were three measurements suitable to estimate the Fried parameter r_0 from the recorded tracking camera videos (see TABLE V.).

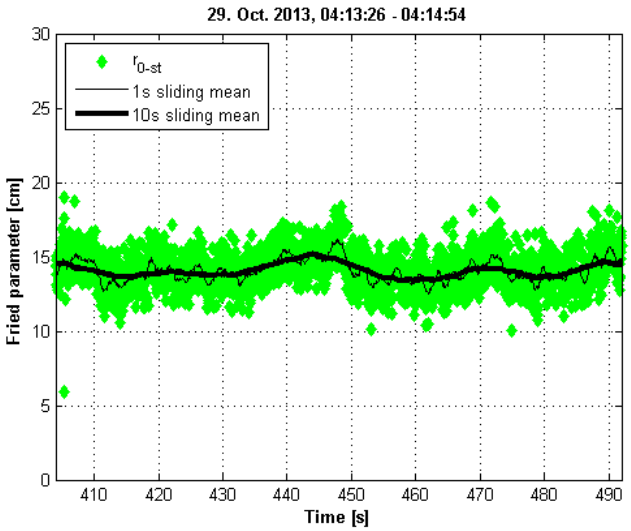

Fig. 12. Example vector of Fried parameter estimation from tracking camera frames, recorded on 29. Oct. 2013.

The measured wavefront data is too small to identify a clear connection between elevation and r_0. However, further improvements to the algorithm used [3] could yield valid results also in the presence of overexposed frames. The available data points (fourth column in TABLE V.) are in good agreement with the values from C_n2-models according to Fig. 9.

TABLE V. MEASURED FRIED PARAMETERS

Date - Time [UTC]	*Record Length [s]*	*Elevation [deg]*	*Mean r_0 [cm]*	*r_0 from models [cm]*
2013-10-26 – 10:12:43	40	38	9.9	7 (IDM)
2013-10-28 – 10:21:59	104	54	8.1	9 (IDM)
2013-10-29 – 04:13:26	88	25	14.1	16 (INM)

V. RESULTS SUMMARY

In the framework of the LOCL-downlink campaign at ESA-OGS on Tenerife, signal-power measurements with 750Hz bandwidth and focal speckle pattern measurements were carried out. Fried-parameter estimations based on the focal-speckle-size method do coincide very well with the Izaña day- and night-models (Fig. 9). Power scintillation values are higher than expected. This is probably due to a small FoV of the sensor together with tracking errors of the telescope.

The LLCD laser downlink campaigns were the first time that the optical free-space transmission channel could be evaluated at a wavelength of 1550nm, as will be used in several future space missions, namely LCRD (NASA), OPALS (JPL), OSIRIS (DLR), and SOTA (NICT).

ACKNOWLEDGMENT

The authors acknowledge the kind support by Hans Smit of ESTEC during the measurement campaigns. We appreciate the opportunity to cooperate with NASA, MIT, and ESA in the frame of the LOCL project.

REFERENCES

[1] D. Boroson, et. al, “Overview and Status of The Lunar Laser Communication Demonstration” Proc. International Conference on Space Optical Systems and Applications (ICSOS) 2012, Corsica, France

[2] Sans, M., Sodnik, Z., Zayer, I. and Daddato, R. Design of the ESA Optical Ground Station for Participation in LLCD Proc. International Conference on Space Optical Systems and Applications (ICSOS) 2012, 2012.

[3] D. Giggenbach, “Deriving an estimate for the Fried parameter in mobile optical transmission scenarios,” Applied Optics, Vol. 50, No. 2,. Optical Society of America, Jan. 2011, p. 222-226

[4] Giggenbach, D., "Optimierung der optischen Freiraumkommunikation durch die turbulente Atmosphäre - Focal Array Receiver," PhD thesis, Universität Der Bundeswehr München (November 2004).

[5] Reyes, M., Alonso, A., Chueca, S., IAC, J. J. F., López, P., Comeron, A., Diós, F., Rodriguez, A., and Rubio, J. A., “ARTEMIS laser link - final report,” Tech. Rep., Instituto de Astrofísica de Canarias (2004).

[6] Andrews, L. and Phillips, R., [Laser Beam Propagation through Random Media], SPIE Press, 2nd edition (2005).